Effect of Li, Ce and Ni on the Corrosion Resistance of Fe_3Al in Molten Na_2So_4 and $NaVO_3$

J. G. González-Rodríguez[1], M. Salazar[2] Luna-Ramírez[3, 5], J. Porcayo-Calderon[3],
G. Rosas[4] and A. Martínez Villfane[5],

[1]*Universidad Autónoma del Estadio de Morelos, FCQI-CIICAP, 62210- Cuernavaca, Mor., México*
[2]*Instituto Mexicano del Petroleo, Eje Central Lazaro Cardenaz, México, D.F., Mexico*
[3]*Instituto de Investigaciones Eléctricas, Cuernavaca, Mor., México*
[4]*Universidad Michoacana de SanNicolas de Hidalgo, Morelia, Mich., Mexico*
[5]*CIMAV, Miguel de Cervantes 120, Chihuahua, Chih., México*

(Received September 2,2003: final form November 5,2003)

ABSTRACT

By using the weight loss technique, the effect of additions of (1.0 at.%) Li, Ni and combinations of Ce+Li and Ce+Ni on the corrosion resistance of Fe_3Al intermetallic alloy in molten salts has been studied. Salts included Na_2SO_4 and $NaVO_3$. Testing temperatures included 600, 650 and 700 °C for $NaVO_3$, and 900, 950 and 1000 °C for Na_2SO_4. All tests were 100 hours long. The corroded specimens were studied in a scanning electronic microscope (SEM). The corrosion products were analyzed with an X-Ray energy dispersive analyzer (EDX) attached to it. In both $NaVO_3$ and Na_2SO_4, corrosion resistance in increased with increasing temperature. The effect of different alloying elements depended upon the salt used. In $NaVO_3$, for instance, the Fe_3Al-base alloy had the highest corrosion rate at 700°C while the Fe_3Al+Ni alloy had the lowest corrosion rate in all temperatures tested. However, in Na_2SO_4 the same alloy, i.e. Fe_3Al+Ni, had the highest corrosion rate and the Fe_3Al-base alloy had the lowest corrosion rate. The results are discussed in terms of the degree of protectiveness that the external Al_2O_3 layer gives to the alloys depending on the testing temperature.

Keywords: Iron aluminide, hot corrosion, weight lost test.

INTRODUCTION

Since one of the main characteristics of iron aluminides is their excellent resistance to different kinds of corrosive attack, it is very important to know their behavior in molten salts environments. The tendency of iron aluminide to form a continuous aluminum oxide (Al_2O_3) layer without the formation of transitory oxides (iron oxides or any oxide from other alloying elements), except under very reductive conditions, suggests that the susceptibility to the attack from species other than oxygen will depend upon the environment to chemically react with the Al_2O_3 layer. In practice, a likely scenario for the corrosive attack is that once the corrosive environment has penetrated towards the substrate, a mechanical damage of the Al_2O_3 layer will follow. Under these circumstances, a repetitive process of formation of the layer is expected /1/. Iron aluminides, based around the compositions Fe_3Al and FeAl, are candidates for high temperature materials because of their excellent oxidation resistance, relatively low cost and density /2-3/. However, the main disadvantage of iron aluminides is their poor ductility, and many efforts have been made to improve their mechanical properties through control of microstructure and alloy composition /4-7/ alloying these materials, for instance, with Li, Ce and Ni /8/.

Some workers have reported the behavior of Fe_3Al alloys in molten salts. However, little has been published on their high-temperature corrosion in molten salt mixtures of V_2O_5-Na_2SO_4. Gesmundo *et al.* /9/ studied the corrosion behavior of Fe_3Al (27 at.% Al-2.2 at.% Cr-0.1 at.% B) and FeAl (40 at.% Al-0.05 at.% Zr-0.06 at.% B-0.085 at.% C) alloys coating by a Na_2SO_4-15wt.%V_2O_5 molten salt in a N_2, 1.0 vol.% O_2, 0.5 vol.% SO_2) simulated combustion gas (at 600°C). They found that after 96 hours of testing, the FeAl alloy showed better corrosion resistance than the Fe_3Al. Tortorelly /3/, when working with Fe_3Al_2Cr intermetallic alloy in molten Na_2SO_4 at 650 and 700°C for 800 hours, found that an aluminum oxide (Al_2O_3) layer plays a very important role in the alloy corrosion resistance. Corrosion of iron aluminides in molten $NaNO_3$(-KNO_3)-Na_2O_2 at 650°C proceeds by oxidation and a slow release from an aluminum-rich product layer into the salt such that the compositions with higher aluminum concentrations yielded significantly better resistance. Recently /10/ Debashis *et al.* studied the effect of carbon (3.7 at.%) on hot corrosion of Fe_3Al in molten Na_2SO_4, finding that the alloy with carbon had a lower corrosion rate than the alloy without carbon because the carbides present along the grain boundaries in the latter hinder the diffusion of sulfur into the material.

Thus, the objective of this work was to evaluate the effect of the additions of minor elements such as Li, Ce and Ni on the hot corrosion performance of the Fe_3Al intermetallic alloy in two commonly found salts in power stations, Na_2SO_4 and $NaVO_3$.

EXPERIMENTAL PROCEDURE

The Fe_3Al alloys were made by conventional gravity casting techniques with pure Fe, Al, Li, Ce using SiC crucibles. The conventional weight loss technique was used to evaluate the resistance of these materials to hot corrosion. The corrosive agents used in the tests were synthetic sodium metavanadate ($NaVO_3$) and pure sodium sulfate (Na_2SO_4). These salts were chosen because they are among the most important compounds found on the deposits formed on the surface of reheater and superheater elements of oil- and coal-fired power stations. Both reagents, i.e. Na_2SO_4 , and $NaVO_3$, were analytical grade. Before corrosion tests, the specimens were cleaned with acetone and dried and then packed in the mixture of salts in porcelain crucibles with 500 mg/cm^2 of the synthetic salt. The corrosion tests were carried out in electric furnaces in static air for 100 hours at temperatures of 600, 650, and 700°C for the case of $NaVO_3$ because its melting point is close to 625°C. Finally, the tests in Na_2SO_4 were performed at 900, 950 and 1000°C, because its melting point is close to 890°C. Two specimens of each condition test were decaled and chemically cleaned according to the ASTM G1 81 standard. One sample of each heat was mounted in bakelite in cross section and polished to analyze the subsurface corrosive attack using scanning electron microscopy (SEM) aided by energy dispersive spectroscopy (EDS) to carry out micro chemical analysis.

EXPERIMENTAL RESULTS

Microstructures

Some of the experimental microstructures for Fe_3Al alloys are shown in Figs. 1-4. Fig. 1 shows the matrix, Fe_3Al, which has coarse precipitates along the grain boundaries. These precipitates turned out to be $AlFe_3C$ according to the X-ray experiments as published elsewhere /8/. With the addition of 1 at.% Ni to the alloy (Fig. 2) the size of the $AlFe_3C$ precipitates was decreased, and when 1 at.% Li was added (Fig. 3), the size of these $AlFe_3C$ phases was drastically decreased. Finally, with the addition of 1 at.% Ce+1 at.% Ni, Fig. 4, a strong formation of the $AlFe_3C$ phase along the grain boundaries occurred, covering large areas.

Hot corrosion results

The effect of temperature on the hot corrosion resistance of the different Fe_3Al intermetallic alloys in $NaVO_3$ is shown in Fig. 5. In all cases it is evident that corrosion rate abruptly increases at 700°C, and that the corrosion rate of the Fe_3Al base material has an intermediate corrosion rate with respect to the alloy with

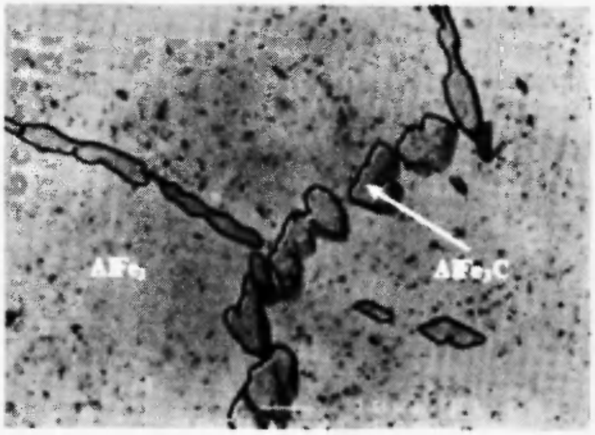

Fig. 1: SEM micrograph of the Fe_3Al alloy showing the presence of $AlFe_3C$ precipitates.

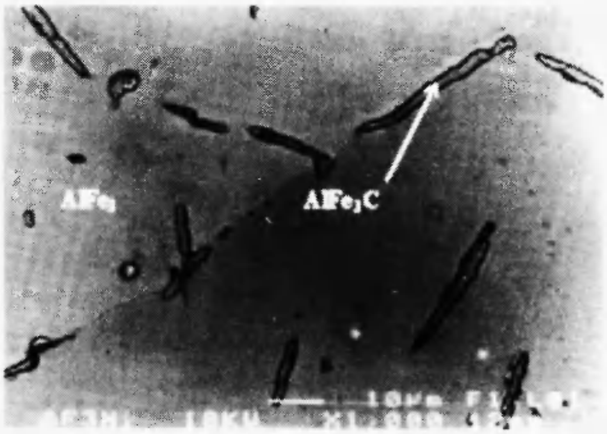

Fig. 2: SEM micrograph of the Fe_3Al +1at.%Ni alloy.

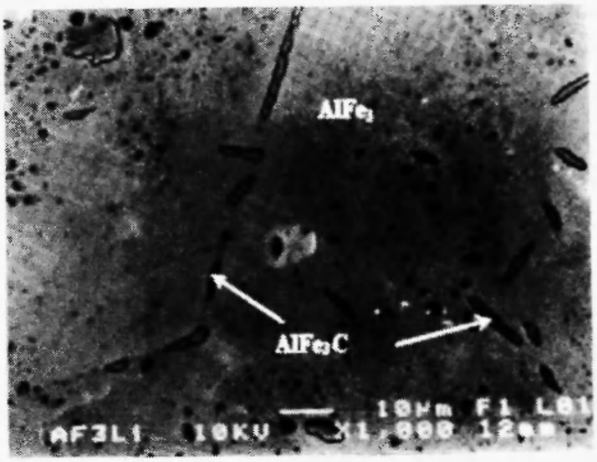

Fig. 3: SEM micrograph of the Fe_3Al +1at.%Li alloy, showing a reduction in the precipitates size.

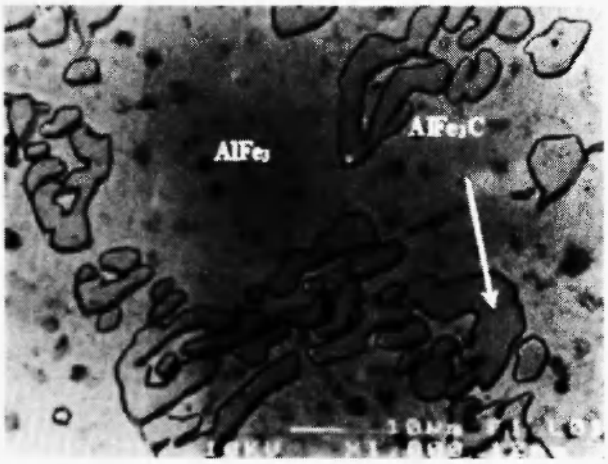

Fig. 4: SEM micrograph of the Fe_3Al +1at.%Ce +1at%Ni alloy, showing large regions of the $AlFe_3C$ phase.

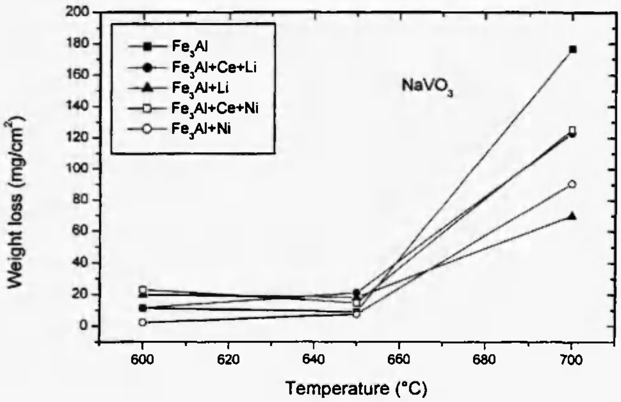

Fig. 5: Effect of Ce, Li and Ni on the corrosion rate of Fe_3Al as a function of temperature in $NaVO_3$.

different alloying elements at 600 and 650°C. At 700°C, however, the Fe_3Al base material was the alloy with the highest corrosion rate. At 600°C, when the salt is still unmelted, for example, the lowest corrosion rate was shown by the Fe_3Al +Ni and the Fe_3Al +Ce+Li alloys, whereas the highest values were exhibited by the Fe_3Al + Ce+Ni and FeAl + Li alloys. At 700°C, however, the lowest corrosion rates were for the Fe_3Al + Li alloy, unlike at 600°C, whereas the highest weight lost was shown by Fe_3Al+Ce+Ni. So, it seems that in all cases the latter had a very rapid deterioration, whereas the FeAl+Ni showed the best resistance to the attack of the

$NaVO_3$ melt. Similarly, in Na_2SO_4, in almost all cases the corrosion rates increased as temperature increased, as shown in Fig. 6. The alloy which had the highest weight lost in all temperatures tested was Fe_3Al+Ni, which in $NaVO_3$ had one of the lowest corrosion rates, whereas one of the alloys with the lowest corrosion rates was the base Fe_3Al. If we compare Figs. 5 and 6, it is clear that the effect of the alloying elements on the corrosion behavior of the Fe_3Al intermetallic alloy is not unique, since the addition of the same element sometimes increases the corrosion rate of the base material in one melt, but in another decreases it.

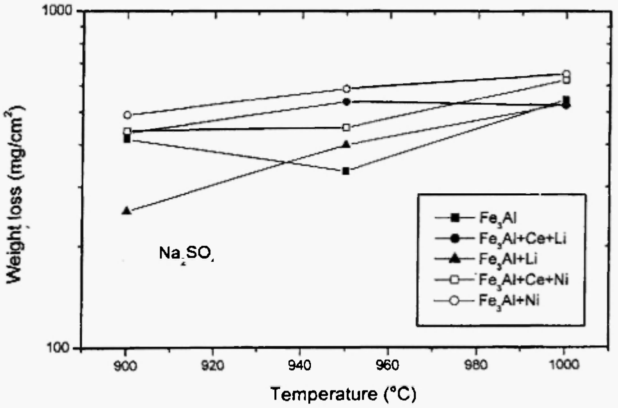

Fig. 6: Effect of Ce, Li and Ni on the corrosion rate of Fe_3Al as a function of temperature in Na_2SO_4.

Micrographs.

A cross section image in the SEM of the FeAl alloy corroded in $NaVO_3$ at 700°C together with X-ray mappings of Al, Fe and V is shown in Fig. 7. It can be seen that on the external layer there is the presence of Al, Fe V and O. Debashis /10/ found that the corrosion products on the external layer of his alloy (Fe_3Al in Na_2SO_4) consisted mainly of alumina (Al_2O_3) with iron oxide (α-Fe_2O_3) as a minor compound. So, it is very likely that aluminum is present as Al_2O_3 whereas iron is present as Fe_2O_3. Vanadium seems to be distributed just beneath the Al_2O_3 layer, which indicates that the molten salt has corroded the external Al_2O_3 layer. Similarly, Fig. 8 shows a cross section of Fe_3Al alloy corroded in Na_2SO_4 at 950°C together with X-ray mappings of Al, Fe, S and O. Again, the presence of Al and Fe on the external layer is clear, showing the presence of Al_2O_3 and Fe_2O_3. There is some evidence of internal sulfidation, since some sulfur was detected inside the alloy.

It is well known that the corrosion rate of an alloy depends upon the degree of protectiveness that the external layer formed by corrosion products on its surface gives to it. If this external layer is protective enough, the corrosion rate is low, but if this layer is not protective at all, then the corrosion rate is high. The Al-based alloys base their corrosion resistance on the establishment of a protective, compact, adherent, aluminum oxide, alumina (Al_2O_3) layer. With the establishment of the Al_2O_3 layer, the corrosion rate should decrease. However, there are different forms of Al_2O_3, and they give different degrees of protection to the alloy. The predominant surface product that forms between 600 and 800°C has been reported to be α-Al_2O_3 /11/ but it is quite possible for γ-Al_2O_3 or θ-Al_2O_3 to exist in this temperature range /12/. These forms of alumina are fast growing, more voluminous, more porous and less protective than α-Al_2O_3 /13/. The temperature at which there is a transition from other types of alumina to the slower growing α-Al_2O_3 appears to be 900°C /13/. This could explain the observed fact of the increase in the corrosion rate with increasing the temperature in $NaVO_3$ and Na_2SO_4 (Figs. 5 and 6) where the testing temperatures were lower than 900°C, and where the predominant external layer is non-protective, fast growing Al_2O_3.

Thus, according to this, and examining the X-ray mappings in Figs. 7 and 8, it seems that the degradation mechanism could start with the oxidation of the alloy and the establishment an external oxide layer (or mixture of oxides, i.e. Fe_2O_3 and Al_2O_3). After this, the oxide layer is dissolved by the molten salt allowing the aggressive elements of the melt (V, S, etc.) to contact the unprotected metal, corroding it, with penetration of some elements like sulfur into the alloy, causing catastrophic corrosion.

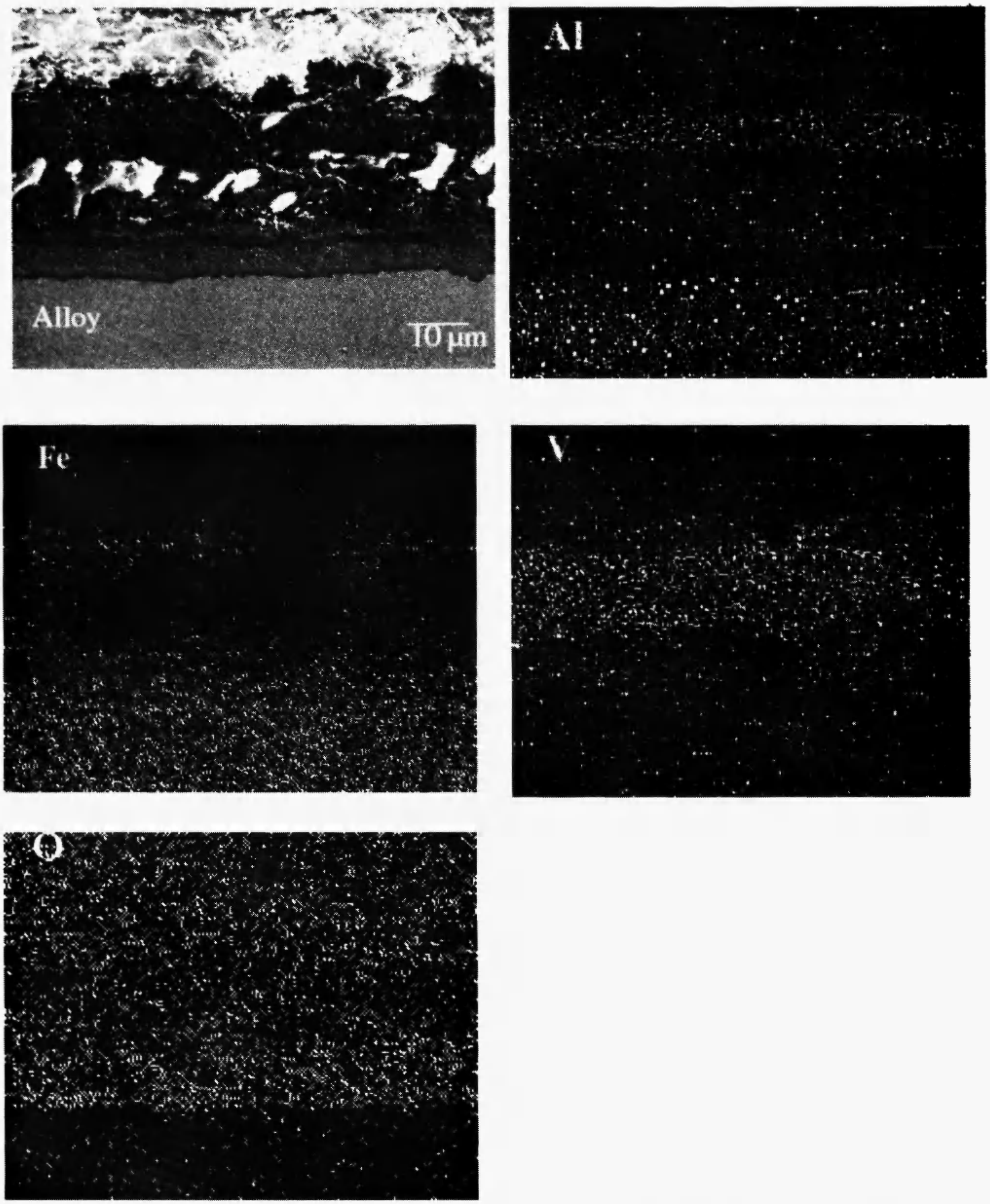

Fig. 7: SEM micrograph of the cross section of the Fe_3Al corroded in $NaVO_3$ at 700°C and X-ray mappings of Al, Fe V and O.

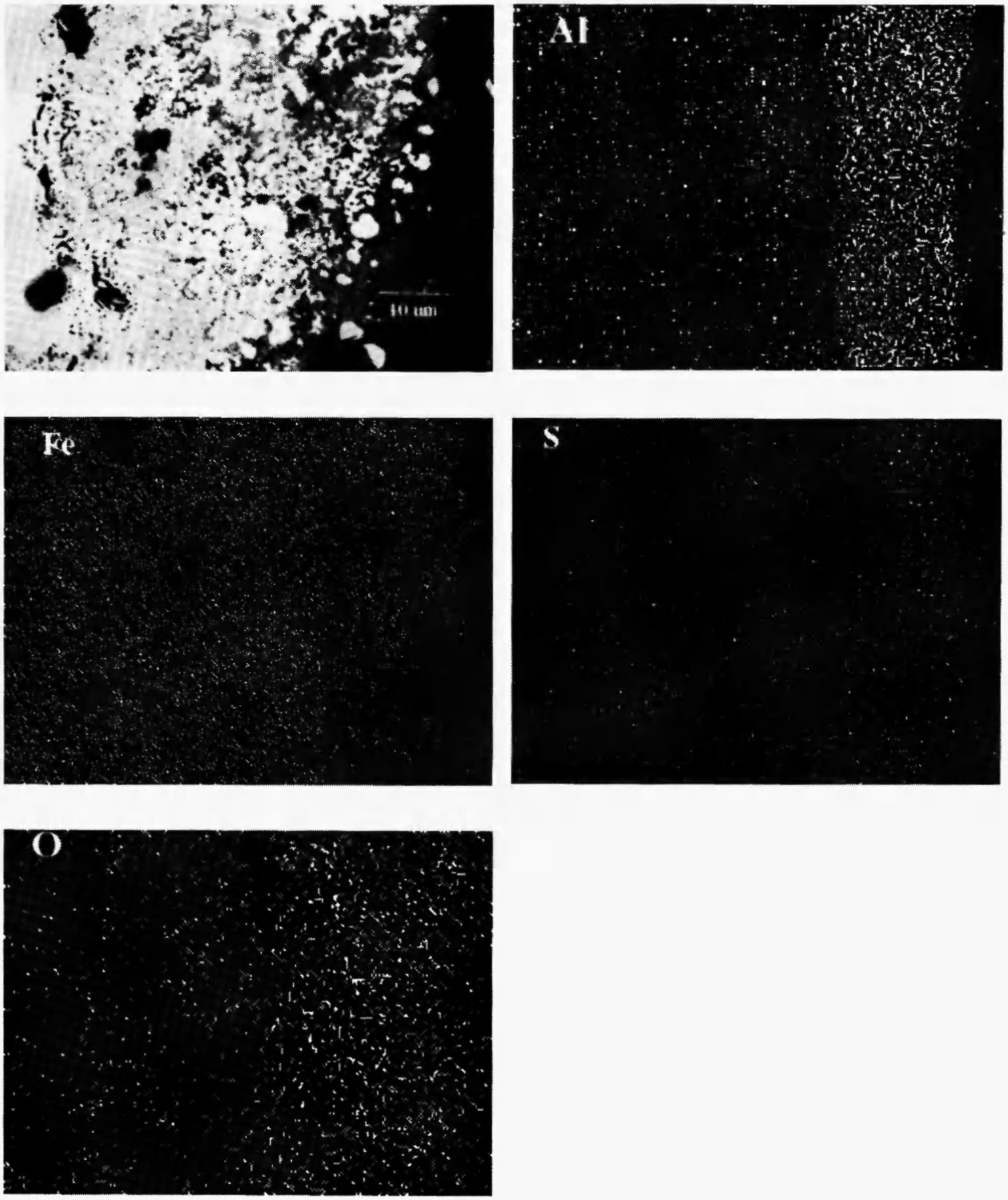

Fig. 8: SEM micrograph of the cross section of the Fe_3Al corroded in Na_2SO_4 at 950°C and X-ray mappings of Al, Fe S and O.

CONCLUSIONS:

The effect of Li, Ni and combinations of Ce+Ni and Ce+Li on the hot corrosion performance of Fe_3Al alloys has been evaluated in $NaVO_3$ and Na_2SO_4 salts using the weight loss technique. From these tests, the following conclusions can be drawn:

1. In both salts $NaVO_3$ and $Na_2SO_4$the corrosion rate increases as temperature increases.
2. The effect of the different alloying elements depends upon the salt used. In $NaVO_3$, the Fe_3Al-base alloy had the highest corrosion rate at 700°C whereas the Fe_3Al+Ni alloy had the lowest corrosion rate in all temperatures tested. However, in Na_2SO_4 the same alloy, i.e. Fe_3Al+Ni, had the highest corrosion rate and the Fe_3Al-base alloy had the lowest corrosion rate. The results are discussed in terms of the degree of protectiveness that the external Al_2O_3 layer gives to the alloys depending on the testing temperature.
3. These results are discussed in terms of the ability of the Al_2O_3 to protect the alloys: at temperatures lower than 900°C, the type of Al_2O_3 formed is not protective, so corrosion rate increases as the temperature increases.

ACKNOWLEDGMENTS:

We are grateful to Ms. Hilda Esparza for her kind assistance in the SEM work.

REFERENCES

1. G. Welsch, J.L Smialek, J. Doychack, J. Waldam and N.S. Jacobson in: *High Temperature Oxidation and Properties,* Chapter 2, G. Welsch and P.D. Desai (Eds.) West Lafayette, IN: Purdue Research Foundation, 1966; p. 121.
2. A. Nishikata and S. Haruyama, *Corrosion*, **42**, 576 (1986).
3. P.F. Tortorelli and K. Natesan, *Mater. Sci. and Eng.*, **A258**, 115 (1998).
4. R. Balasubramaniam, *J. Alloys Compounds,* **253-254**, 148 (1997).
5. C.T. Liu, E.P. George, P.J. Maziasz, J. H. Schneibel, *Mater. Sci. and Eng.*, **A258**, 84 (1998).
6. V.K. Sikka, D. Wilkening, J. Liebetrau and B. Mackey, *Mater. Sci. and Eng.*, **A258**, 229 (1998).
7. Z. Zhongua, S. Yangshan, G. Jun, W. Kunzhong, *J. Rare Earths* **14**(2), 145 (1996).
8. M. Salazar, A. Albiter, G. Rosas and R. Perez, *Mater. Sci. and Eng.*, **A351**, 154 (2003).
9. F. Gesmundo, Y. Niu, F. Viani and O. Tassa, *Journal de Physique IV*, **3**, 375 (1993).
10. D. Deabashis, R. Balasubramaniam and M.N. Mungole, *Mater. Sci. and Eng.*, **A351**, 154 (2003).
11. M. Sakiyama, P. Thomaszeweiz and G.R. Wallwork, *Oxid. Met.* **13**, 311 (1979).
12. B. A. Pint, in: D.A. Shores, R.A. Rapp, P.Y. Hou (Eds.), *Fundamental Aspects of High Temperature Corrosion,* The Electrochemical Society, Pennington, N.J. 1997; p.74.
13. K. Natesan, *Mater. Sci. Eng.* **A258**, 126 (1998).